

# Inverse proximity effect in superconductors near normal or ferromagnetic material

M. A. Sillanpää,<sup>1,\*</sup> T. T. Heikkilä,<sup>2,3</sup> R. K. Lindell,<sup>1</sup> and P. J. Hakonen<sup>1</sup>

<sup>1</sup>*Low Temperature Laboratory, Helsinki University of Technology P.O.Box 2200, FIN-02015 HUT, Finland*

<sup>2</sup>*Materials Physics Laboratory, Helsinki University of Technology P.O.Box 2200, FIN-02015 HUT, Finland*

<sup>3</sup>*Institut für Theoretische Festkörperphysik, Universität Karlsruhe, D-76128 Karlsruhe, Germany*

We study the electronic density of states in mesoscopic superconductors near a transparent interface with either a non-magnetic normal metal or a ferromagnetic metal. In our tunnel spectroscopy experiment, a substantial density of states is observed at sub-gap energies close to a ferromagnet. This effect of smearing of the superconductor density of states is weak in the case of the non-magnetic metal. We compare our data with calculations based on the Usadel equation, where the effect of the ferromagnet is treated as an effective boundary condition. For the ferromagnetic case we obtain a good agreement, but the weak effect of the non-magnetic metal is inconsistent with theoretical predictions.

A number of experiments have investigated the proximity effect in superconducting - normal mesoscopic structures [1]. In normal (N) metals, the proximity effect has the decay length  $\xi_N = \sqrt{\hbar D/2\pi k_B T}$  which is set by the dephasing of correlations between electrons and Andreev-reflected holes having slightly different momenta. At typical experimental conditions at low temperatures, the effect can survive up to large distances of several hundred nanometers. The experiments in non-magnetic metals have been generally well understood within the framework of the quasiclassical theory of inhomogeneous superconductivity.

On the other hand, the interplay between superconducting (S) and ferromagnetic (F) materials has remained elusive. There have been fewer experiments in mesoscopic SF structures, and some of them remain in contradiction with theory. Some recent experiments [2, 3, 4, 5, 6] appear to indicate the existence of a long-range (i.e. a penetration depth comparable to  $\xi_N$ ) proximity effect into a ferromagnet. This interpretation is in contradiction with the fact that the Cooper pair amplitude diffusing into a ferromagnet should decay over microscopic distances  $\xi_F = \sqrt{\hbar D/2\pi k_B T_{\text{Curie}}}$  due to the considerable difference in the momenta of spin-up and spin-down quasiparticles. A spectroscopy experiment in a low- $T_{\text{Curie}}$  ferromagnet [7] agreed with the theoretical picture of a short-range effect. Here we report measurements on an inverse phenomenon, the modification of the BCS density of states in mesoscopic superconducting strips of Al under the influence of the proximity effect of a ferromagnet (Ni). Moreover, we confront the previously well-tested quasiclassical theory with a similar experimental condition, but with a non-magnetic normal metal (Cu).

We use tunnel spectroscopy with tunnel probes at fixed positions to measure the differential conductance on the S side of the interface. At zero temperature, and in the absence of Coulomb effects at the tunnel contact, the

differential conductance  $G(E)$  with an N metal probe is proportional to the density of states (DOS). This way we can probe how the DOS in a superconductor is affected by the proximity effect. An experiment analogous to ours, with non-magnetic N metal but on the N side, has been performed by Gueron *et al.* [8], who have observed a dip in the N metal DOS up to one  $\mu\text{m}$  from the interface. On the S side of SN proximity systems, the DOS has been investigated previously by STM in short-coherence length layered superconductors [9, 10, 11], and recently in Nb-Au structure [12], but no quantitative comparisons to theoretical predictions have been made.

We used a sample structure shown in the inset of Fig. 2. In the samples, we have two tunnel spectroscopy probes: one at a distance of approximately 180 nm from the transparent SN (or SF) interface (called the interface junction), and one 10  $\mu\text{m}$  from the interface (called the bulk junction). The latter tunnel junction is assumed to be located at a site with properties of bulk Al. We made two samples at different chips, one where Al was in contact to Cu (labelled sample A), and one where Al was in contact to Ni (sample B). The samples were fabricated on oxidized Si wafers by electron beam lithography and shadow evaporation through PMMA/MMA copolymer mask. We first evaporated 20 nm of Al. To make the clean SN interface, we evaporated a 25 nm layer of Cu at a different angle (sample A). For sample B, Ni was evaporated instead. The depositions of the first two layers were done in a single UHV cycle at pressures below  $5 \cdot 10^{-9}$  mBar, avoiding any delay between the successive layers to make a transparent interface. The Al wires were then oxidized in 0.3 mBar of  $\text{O}_2$  for 5 minutes in order to make the opaque barriers for tunnel spectroscopy. Lastly, the tunnel probes were made by depositing 40 nm of Cu at a third angle. The process yielded resistances of approximately 20  $\text{k}\Omega$  for both tunnel junctions in sample A, and 1.5  $\text{M}\Omega$  in sample B.

For electric transport measurements, the samples were cooled down to approximately 100 mK in a plastic dilution refrigerator. Conductance measurements for the tunnel probes were performed through carefully filtered coaxial leads. To measure differential conductance, we

\*Mika.Sillanpaa@iki.fi

used lock-in techniques with 20-30  $\mu\text{V}$  ac excitation added to a constant dc voltage bias applied to the tunnel probe to be measured. Whether the measurement current was put to go through either terminal (1) or terminal (2) (inset of Fig. 2), did not have any appreciable effect on the tunnel conductance.

The tunnel spectra of both samples exhibited qualitatively similar behavior. We obtained a BCS-like differential conductance for the bulk junction, although the BCS peaks were somewhat lower than what would be expected simply by thermal broadening. The magnitude of the peaks was accurately accounted for only when we took into account the Coulomb charging effects (see below). For the interface junction, the peaks were lower, with a clear sub-gap conductance. For sample B (nickel), the increase of resistance near zero bias was smaller by a factor of five as compared with sample A; hence the superconducting gap was substantially more suppressed near Ni than near Cu (Fig. 1).

In the normal state, superconductivity being suppressed by perpendicular magnetic field, we observed a typical conductance dip around small bias due to Coulomb charging effects. In sample A, in both tunnel probes, the dip was only 10 % of total conductance, whereas sample B, both probes, showed a dip of nearly 40 % due to a resistive environment created by the relatively resistive nickel wires.

Diffusion constants for the wires or the interface resistance were not directly measurable in the samples. We used test samples, made in a similar process, to measure resistivities for thin wires of Al, Ni and Cu, with the results  $\rho_{\text{Al}} = 1.7 \mu\Omega\text{cm}$ ,  $\rho_{\text{Cu}} = 2.0 \mu\Omega\text{cm}$  and  $\rho_{\text{Ni}} = 32 \mu\Omega\text{cm}$ . For Al, the coherence length is thus  $\xi_S = \sqrt{\hbar D/2\Delta} \simeq 150 \text{ nm}$ . For sample A, an upper bound for the normal-state interface resistance  $R_B$  of approximately  $R_B < 50 \Omega$  was estimated from resistance measurement between the tunnel probe and point (1) in Fig. 1. For sample B, a separate test sample was used to measure the SF interface resistance, with the result  $R_B \simeq 40 \Omega$ .

The density of states near an SN (SF) interface can be calculated from the Usadel equation [13] for the quasiclassical Green's functions in the diffusive limit. These functions can be parametrized using the  $\theta$ -parametrization [14]. In the absence of supercurrents the retarded Green's function is  $\hat{G}^R = \cosh(\theta)\hat{\tau}_3 + i \sinh(\theta)\hat{\tau}_2$ , where  $\hat{\tau}_i$  are the Pauli matrices in Nambu space. In the case of translational invariance in the transverse directions, the Usadel equation then takes the form

$$D\partial_x^2\theta = -2iE\sinh(\theta(E, x)) + 2i\Delta(x)\cosh(\theta(E, x)). \quad (1)$$

Here  $D$  is the diffusion constant and  $\Delta(x)$  is the superconducting pair potential, which is calculated self-consistently from

$$\Delta(x) = \lambda N_0 2\pi T \sum_{\omega_n} \sinh \theta(\omega_n, x), \quad (2)$$

where  $N_0$  is the density of states in the normal state, and the sum goes over the discrete Matsubara frequencies  $\omega_n = (2n + 1)\pi T$  and is cut off at the Debye energy. The attractive interaction between the electrons is characterized by the coupling parameter  $\lambda$ , which is a nonzero constant for superconducting materials and zero otherwise. The parameter  $\theta(\omega_n, x)$  is calculated from Eq. (1), where the energy  $E$  is replaced by  $i\omega_n$ .

Since the interface between the two materials is not ideal in the experiments, Eqs. (1,2) have to be complemented by a boundary condition recently derived by Nazarov [15], relating the Green's function in the left side of the interface ( $\hat{G}_1 = \hat{G}(x = 0^-)$ ) to the function in the right side ( $\hat{G}_2 = \hat{G}(x = 0^+)$ ),

$$\sigma_1 \hat{G}_1 \partial_x \hat{G}(0^-) = \sigma_2 \hat{G}_2 \partial_x \hat{G}(0^+) = \frac{e^2}{h} \sum_n 2T_n \frac{[\hat{G}_2, \hat{G}_1]}{4 + T_n (\{\hat{G}_2, \hat{G}_1\} - 2)}. \quad (3)$$

We assume identical normal-state conductivities  $\sigma_1 = \sigma_2 = \sigma_N$  and equal cross sections  $A$  of the wires (measurements indicate only about a 15% difference between the normal-state conductivities in the NS case where these are relevant). In a junction with many transmission channels, the distribution of the transmission eigenvalues  $T_n$  can be obtained from random matrix theory [16]. In the case of a dirty interface it is given by [17]

$$\rho(T) = \frac{1}{\rho_B e^2} \frac{1}{T^{3/2} \sqrt{1 - T}}, \quad (4)$$

where  $\rho_B$  is the normal-state resistance of the interface per unit area. Integrating Eq. (3) over the distribution of eigenvalues and over the cross sections of the wires, we finally get the desired boundary condition

$$\partial_x \theta(0^+) = \partial_x \theta(0^-) = \frac{\sqrt{2}}{r_b} \frac{\sinh(\theta(0^+) - \theta(0^-))}{\sqrt{1 + \cosh(\theta(0^+) - \theta(0^-))}} \quad (5)$$

where  $r_b = R_B/R_\xi$  is the ratio between the normal-state resistance  $R_B = \rho_B A_B$  of the interface with the cross section  $A_B$ , and the resistance  $R_\xi = \xi/\sigma_N A$  of a piece of wire with length  $\xi$  the cross section  $A$ .

From the solution  $\theta(E, x)$  to Eqs. (1,2,5), we obtain the local density of states through

$$N(E, x) = N_0 \text{Re}\{\cosh(\theta(E, x))\}. \quad (6)$$

In Figs. 2 and 3 we plot the DOS at varying values of the interface transparency  $r_b$  and at varying distances to the interface. At high interface transparency, the gap is substantially more suppressed in SF structures than in SN structures. At low transparency, the main difference between N and F is the small dip in N around zero, which comes due to the finite length of the calculated phase-coherent wire and which in experiments would easily be smeared by the temperature.

To calculate differential conductance of a tunnel probe, we have to take into account Coulomb charging effects due to the smallness of the tunnel junction capacitance. The charging effects depend on the impedance of the electromagnetic environment in terms of the function  $P(E)$  which is the probability of exchange of energy between the tunneling electron and the environment. Forward tunneling rate through a single junction having the tunnel resistance  $R_T$  is given by [18]

$$\Gamma(V) = \frac{1}{e^2 R_T} \int_{-\infty}^{+\infty} dE dE' \frac{N_0 N_S (E' + eV)}{N_0^2} \times (7)$$

$$f(E)[1 - f(E' + eV)]P(E - E'),$$

where  $N_0$  is DOS of the tunnel probe, taken as constant, and  $N_S$  is the proximity-affected DOS on the S side. The function  $P(E)$  is calculated from an integral equation assuming a purely resistive environment [19].

For both samples and each tunnel probe, the parameters  $\alpha = R_Q/R_{\text{env}}$  and the charging energy of tunnel junction capacitor  $E_C$  were determined as the values that gave the best fit to the normal-state conductance. Here,  $R_Q = h/4e^2 \simeq 6.5 \text{ k}\Omega$  is the superconducting resistance quantum, and  $R_{\text{env}}$  is the resistance of the electromagnetic environment seen by the tunnel junction. Normal-state data of both junctions in a given sample were fitted with the same values. For sample B, these values were then used to fit  $\Delta$  in bulk Al data, and we obtained a faultless fit with  $\Delta \simeq 0.22 \text{ mV}$  and with the temperature  $T = 100 \text{ mK}$  that was recorded in the experiment. For sample A, the Al/Cu sandwiches on the chip apparently turned superconducting, and the best fit for bulk Al was obtained with a vanishing resistance of the environment. Moreover, because of a relatively small tunnel junction resistance, heating effects of the bias current at the measurement temperature  $T = 130 \text{ mK}$  became significant, and a good fit was obtained only with an elevated temperature of  $260 \text{ mK}$ .

The distance between the interface and the first probe in both samples had some ambiguity of  $\pm 50 \text{ nm}$  because the tunnel probes had a finite width of  $80 \text{ nm}$ , and because the two metal films at the interface overlapped each other approximately  $50 \text{ nm}$ . Average of the DOS over these distances was practically equal to the DOS in the middle of the tunnel probe, and we used the average distance (this distance is about  $1.2 \xi_S$ ) in the analysis.

All the previously determined parameters were used to fit the conductance of the interface junction with the remaining parameter, the interface transparency  $r_b$ . With  $R_\xi \simeq 17 \Omega$  and  $R_B \simeq 40 - 50 \Omega$ , we would expect  $r_b \simeq 3$ .

In the case of the Ni sample (B), we indeed obtained an excellent fit with  $r_b = 3$ .

For the Cu sample (A), the predicted sub-gap conductance remains too large by a factor of five at  $r_b = 3$ . Also the predicted gap is too small by approximately 10 %. We emphasize that this data can not be explained with different values for those parameters that have not

been determined precisely, namely  $r_b$  and  $\xi_S$ . With a smaller  $\xi_S$  (and hence a larger effective distance from the interface) we could fit the sub-gap region, but the BCS peaks would become too sharp, which rules out this possibility. A similar problem arises when  $r_b > 3$  and the BCS peaks grow too sharp when the coupling between S and N gets weaker; in any case, values of  $r_b$  larger than approximately 3 are unlikely because of the estimated upper bound for  $R_B$ . To check for further possibilities, we explored with values of temperature,  $\alpha$  or  $E_C$  different from those determined by our initial fitting procedure, but we could not obtain any better agreement.

In conclusion, we have measured the inverse proximity effect in mesoscopic superconductors in contact with either Cu or Ni, and compared the data with a detailed model based on the Usadel equation. The case of Ni is well described by theory, but there are significant deviations between data and theoretical results in the effect of Cu.

## Acknowledgments

The authors would like to thank Monique Giroud and Wolfgang Belzig for useful ideas and comments. This research was supported in part by Emil Aaltonen foundation, and by the Human Capital and Mobility Program ULTI of the European Union.

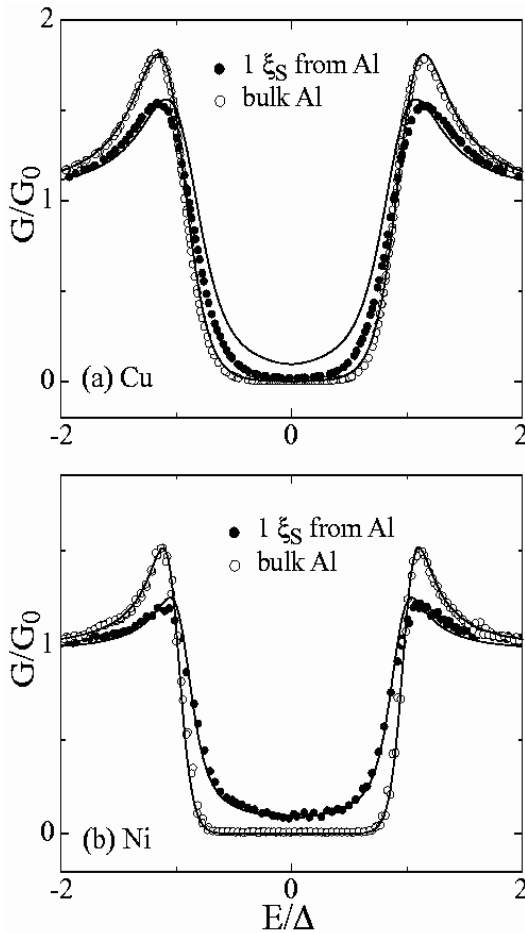


FIG. 1: Normalized differential conductance  $G/G_0$  of SIN junctions, when properties of S are affected by proximity of a ferromagnet or a non-magnetic normal metal. The circles are the experimental data at a distance of 180 nm ( $1.2 \xi_S$ ) from the interface, and that for the bulk Al, shown for reference. The data are normalized to the conductance value  $G_0$  measured at 1 mV. The solid curves are the best fits to theory. (a) N metal is copper (non-magnetic), measured at  $T = 130$  mK. The theoretical curves were fitted with the values  $\alpha = R_Q/R_{\text{env}} = 30$  (implying  $R_{\text{env}} = 220 \Omega$ ),  $E_C/k_B T = 9$ ,  $E_C = \Delta$ ,  $r_b = 3$ , and a higher temperature  $T = 260$  mK due to bias current heating; (b) N metal is a ferromagnet (nickel) at  $T = 100$  mK. In the theoretical curves, the values  $\alpha = 7.5$  ( $R_{\text{env}} = 870 \Omega$ ),  $E_C/\Delta = 1.5$ ,  $r_b = 3$ , were used. The gap of Al was  $\Delta = 0.22$  mV in both samples.

[1] See e.g. H. Courtois, Ph. Gandit and B. Pannetier, Phys. Rev. B **52**, 1162 (1995); H. Courtois, Ph. Gandit, D. Mailly, and B. Pannetier, Phys. Rev. Lett. **76**, 130 (1996); V. N. Antonov, A. F. Volkov, and H. Takayanagi, Phys. Rev. B **55**, 3836 (1997).

[2] V. T. Petrashov, V. N. Antonov, S. V. Maksinov, and R.

Sh. Shaikhaidarov, JETP Lett. **59**, 551 (1994).  
 [3] M. Giroud *et al.*, Phys. Rev. B **58**, 11872 (1998).  
 [4] V. T. Petrashov *et al.*, Phys. Rev. Lett. **83**, 3281 (1999).  
 [5] V. T. Petrashov *et al.*, J. Low Temp. Phys. **118**, 689 (2000).  
 [6] V. T. Petrashov *et al.*, cond-mat/0005437.

- [7] T. Kontos, M. Aprili, J. Lesueur, and X. Grison, Phys. Rev. Lett. **86**, 304 (2001);
- [8] S. Gueron et al, Phys. Rev. Lett. **77**, 3025 (1996).
- [9] S. H. Tessmer, D. J. Van Harlingen, and J. W. Lyding, Phys. Rev. Lett. **70**, 3135 (1993).
- [10] S. H. Tessmer *et al.*, Phys. Rev. Lett. **77**, 924 (1996).
- [11] A. D. Truscott, R. C. Dynes, and L. F. Schneemeyer, Phys. Rev. Lett. **83**, 1014 (1999).
- [12] N. Moussy, H. Courtois, and B. Pannetier, unpublished.
- [13] K. D. Usadel, Phys. Rev. Lett. **25**, 507 (1970).
- [14] W. Belzig *et al.*, Superlattices Microstruct. **25**, 1251 (1999).
- [15] Yu. V. Nazarov, Superlattices Microstruct. **25**, 1221 (1999).
- [16] W. Belzig, A. Brataas, Yu. V. Nazarov, and G. E. W. Bauer, Phys. Rev. B **62**, 9726 (2000).
- [17] K. M. Schep and G. E. W. Bauer, Phys. Rev. Lett. **78**, 3015 (1997).
- [18] G.-L. Ingold and Yu. Nazarov, in *Single Charge Tunneling*, edited by M. H. Devoret and H. Grabert (Plenum, New York, 1992).
- [19] G.-L. Ingold, and H. Grabert, Europhys. Lett. **14**, 371 (1991).

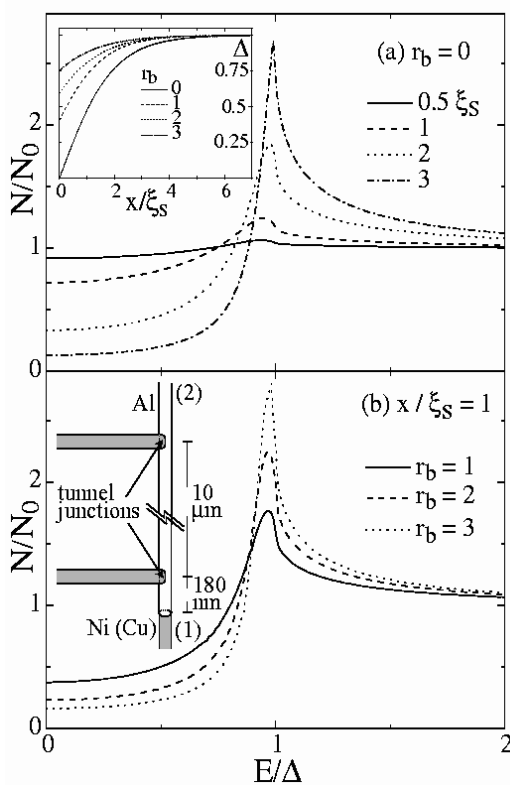


FIG. 2: DOS of SF structures calculated on the S side, (a) with an ideal interface  $r_b = 0$ , at distances  $0.5 \xi_S \dots 3 \xi_S$  from the interface; (b) at a fixed distance  $1 \xi_S$  with varying interface transparencies  $r_b = 1 \dots 3$ . In the calculations, the S order parameter was assumed not to penetrate F, i.e. DOS in F was taken as constant  $N_0$ . The insets show the self-consistent pair potential and schematics of the sample.

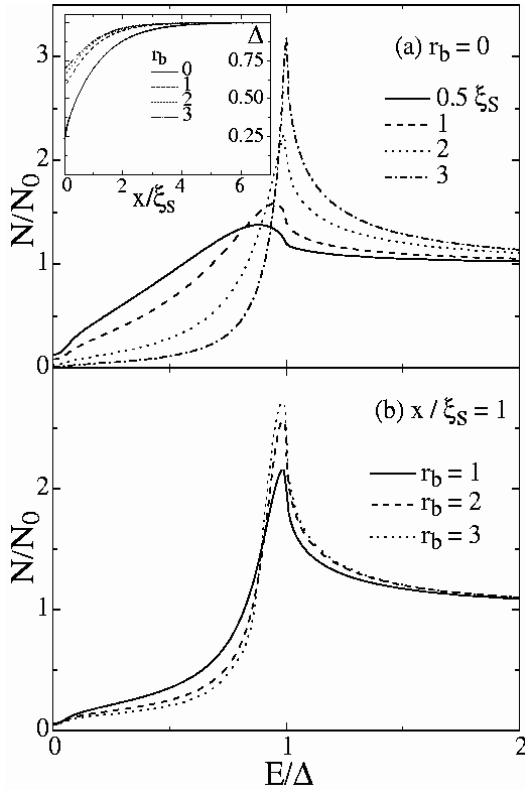


FIG. 3: DOS calculated on the S side near SN interface, (a) with an ideal interface  $r_b = 0$  at distances  $0.5 \xi_S \dots 3 \xi_S$  from the interface; (b) with varying interface transparencies  $r_b = 1 \dots 3$  at a fixed distance of  $1 \xi_S$ . In the insets are shown the self-consistent pair potentials for the same  $r_b$  values.